

# Soil-Structure System Identification of Millikan Library North–South Response during Four Earthquakes (1970–2002): What Caused the Observed Wandering of the System Frequencies?

by Maria I. Todorovska

**Abstract** An application is presented of a recently proposed system identification method for buildings that takes into account the effects of soil-structure interaction and the coupling of the horizontal and rocking motions of the foundation. The method gives the uncoupled structural fixed-base frequency  $f_1$  and rigid-body rocking frequency  $f_R$  using data only from two horizontal sensors (at base and roof). The fixed-base frequency is estimated from the wave travel time through the structure, the apparent system frequency from Fourier analysis, and the rocking frequency from a relation between these three. The case study is Millikan Library in Pasadena, California. Results are shown for four earthquakes between 1970 and 2002. The method makes it possible to quantify the degree to which the observed changes (wandering) of its resonant frequencies have been due to changes in the structure alone. The results show that (1) both  $f_1$  and  $f_R$  are amplitude dependent, (2) significant permanent reduction of frequency occurred over the years,  $\sim 22\%$  for  $f_1$  and  $11\%$  for the apparent frequency  $f_{1,app}$ , mostly caused by the San Fernando earthquake of 1971, while (3) the changes of  $f_R$  have been amplitude dependent and recoverable. (4) During the San Fernando earthquake, both  $f_1$  and  $f_R$  dropped, respectively, by  $\sim 24\%$  and  $\sim 18\%$ , resulting in  $21\%$  drop of  $f_{1,app}$ . (5) After this earthquake, the changes in the observed resonant frequencies, which are those of the system, have been due to a much larger degree (4–5 times) to changes of  $f_R$  than to changes of  $f_1$ . (6) The small permanent changes in  $f_1$  that appear to have occurred after the San Fernando earthquake cannot be deciphered with certainty because of the small number of earthquake records available for this analysis since 1971. Records from the period 1988 to 2002, when released, can be used in future to refine and verify these trends.

## Introduction

Long-term seismic monitoring of structures has demonstrated that their resonant frequencies of vibration (as determined by Fourier analysis, which are those of the soil-structure system and depend on the properties of the structure, soil and foundation) can vary significantly from one earthquake to another and with time. Udvardia and Trifunac (1974) showed that these frequencies drop during strong shaking but recover partially or totally. Recoverable changes, not related to damage, appear to reach and exceed  $20\%$  (Trifunac *et al.*, 2001a,b; Todorovska *et al.*, 2006). Unfortunately, for the majority of significant recordings, it has been difficult to tell to what degree the observed changes have been due to change of the properties of the soil and foundation as opposed to the structure because of inadequate instrumentation to separate the effects of the soil-structure interaction. For the same reason, it has been also difficult to estimate, directly from earthquake observations, the fixed-

base frequencies of the structure. Distinguishing between fixed-base and system frequency is important because the observed frequencies are often erroneously used to calibrate the stiffness of structural models and using system frequency for such purpose leads to underestimation of the structural stiffness. Distinguishing between the two sources of non-linear behavior (in structure and soil) and of the change of the relevant frequencies is important for structural health monitoring because the changes in system frequency are often used erroneously to infer the change in the health of a structure.

Recently, Todorovska (2009) showed how both the building fixed-base frequency  $f_1$  and rigid-body rocking frequency  $f_R$  can be estimated using earthquake response data from only two horizontal sensors, one at the roof and the other one at the base extending the usability of structural response data from past earthquakes. This method is based on

measuring the wave travel time from the base to the top of a building using impulse response functions (Snieder and Şafak, 2006) and on a relationship between  $f_1$ ,  $f_R$ , and  $f_{1,app}$ , where  $f_{1,app}$  is the system resonant frequency obtained from transfer-function between the roof and base horizontal responses, which assumes rigid foundation (Luco *et al.*, 1987). This article presents an application of the method described in Todorovska (2009) to the north–south earthquake response of Millikan Library during four earthquakes for which data were available for both basement and roof response. Millikan Library is a nine-story reinforced concrete (RC) building in Pasadena, California, instrumented over a long period of time (for 40 yr) and tested extensively. Structural deformation patterns obtained from detailed ambient vibration tests showed that for its north–south response, rigid foundation model may be appropriate, and that as much as 30% of its roof response can be accounted for by the rigid-body rocking, suggesting significant soil-structure interaction effects (Foutch *et al.*, 1975; Luco *et al.*, 1987). Its vibrational properties have been identified from forced vibration test data, considering the effects of soil-structure interaction (Luco *et al.*, 1986, 1987, 1988; Wong *et al.*, 1988), which provides an independent reference point to compare the results of this study. The San Fernando (SF) 1970 earthquake produced a significant drop of  $f_{1,app}$  (Udwadia and Trifunac, 1974), which did not recover completely to its preearthquake value. The cause of the permanent change has been attributed to degradation of the structural stiffness based on ambient and forced vibration tests before and after this earthquake (Luco *et al.*, 1987). Since the 1971 earthquake, smaller drops of its system frequencies have been observed over time in data from many forced vibration tests, documented most recently in Clinton *et al.* (2006). These results represent other independent reference to check the consistency of the results in this article, which are based entirely on earthquake records. Clinton *et al.* (2006) also documented the variability, which they termed wandering of the resonant (i.e., system) frequencies of the building for ambient noise excitation due to environmental effects (strong winds, heavy rainfall, and temperature) and changes in mass. Finally, wave propagation through the building has also been studied for small earthquake excitation (Yorba Linda [YL] 2002 earthquake) and wave travel times through the structure for north–south motions have been measured using impulse response functions by Snieder and Şafak (2006). However, their identified building fixed-base frequency is in fact  $f_{1,app}$  (Todorovska, 2009).

In this article, the wave travel time  $\tau$  (from the ground to the top of the building) is measured as in Snieder and Şafak (2006), but the fixed-base frequency is estimated by  $f_1 = 1/(4\tau)$  as in (Todorovska, 2009), assuming that the building deforms primarily in shear. The rigid-body rocking frequency  $f_R$  is also estimated. The emphasis of the analysis is on the changes of  $f_1$ ,  $f_R$ , and  $f_{1,app}$  with amplitudes of response, time, and relative to each other. A comparison is shown of the system transfer-functions and impulse response functions for the model in Todorovska (2009) and those

obtained from records of the Yorba Linda earthquake of 2002. The results show that during the San Fernando 1971 earthquake, both  $f_1$  and  $f_R$  dropped ( $f_1$  by 24% and  $f_R$  by 18%). Because of this earthquake, permanent change of  $f_1$  occurred, while  $f_R$  recovered. After this earthquake, the changes in  $f_1$  and  $f_R$  are amplitude dependent and recoverable (within the accuracy of the method and limited number of earthquakes studied) with the percentage change of  $f_R$  being much greater than the percentage change of  $f_1$ .

Estimates of fixed-base frequency  $f_1$  as  $1/(4\tau)$  and of soil-structure system frequency  $f_{1,sys}$  (from Fourier analysis) obtained from earthquake response data have been compared for three buildings, and it was shown that  $f_1 = 1/(4\tau) > f_{1,sys}$ , confirming that  $1/(4\tau)$  is a physically meaningful estimate of  $f_1$  for the cases considered (Todorovska and Trifunac, 2008a, b; Trifunac *et al.*, 2008). Further, Kawakami and Oyunchimeg (2004) compared  $1/(4\tau)$  with fixed-base frequency from modal analysis for a theoretical model of a 10-story frame and showed that  $1/(4\tau)$  is a good estimator of  $f_1$  if the stiffness is distributed uniformly along the building height.

## The Building and Data

Millikan Library is a 9-story RC building located in Pasadena, California, instrumented since 1967. Detailed description of the structure and its foundation can be found in Luco *et al.* (1986); Wong *et al.* (1988) and Clinton *et al.* (2006) and is repeated here for completeness. It has plan dimensions  $21 \times 23$  m and vertically extends 43.9 m above grade and 48.2 m above the basement slab. Resistance to lateral forces in the north–south direction is provided mainly by 30 cm RC shear walls on the east and west sides of the building. The 30 cm RC central core houses the elevators and provides most of the resistance to lateral forces in the east–west direction. The foundation system is composed of a central pad 9.75 m wide by 1.2 m deep, which runs in the east–west direction and extends across the building between the curved shear walls at the east and west ends. Also provided are beams 3 m wide by 0.61 m deep, which run east–west beneath the rows of columns at the north and south ends of the building. These beams are connected to the central pad by stepped beams. The contact between the central pad and the underlying soil is approximately 7 m below the first floor level. The plan dimensions of the foundation are approximately  $23.3 \times 25.1$  m with additional areas of dimensions  $9.9 \times 1.7$  m and  $9.9 \times 3.5$  m at the east and west extremes, respectively. The local soil can be characterized as alluvium with average shear wave velocity in the top 30 m of about 300 m/sec and depth to bedrock of about 275 m. The alluvium consists of medium to dense sands mixed with gravels, and the water table appears to be at about 11 m depth. Figure 1 shows (a) photo of the building, (b) north–south cross section, (c) typical floor plan, and (d) basement showing the location of the sensors and orientation.

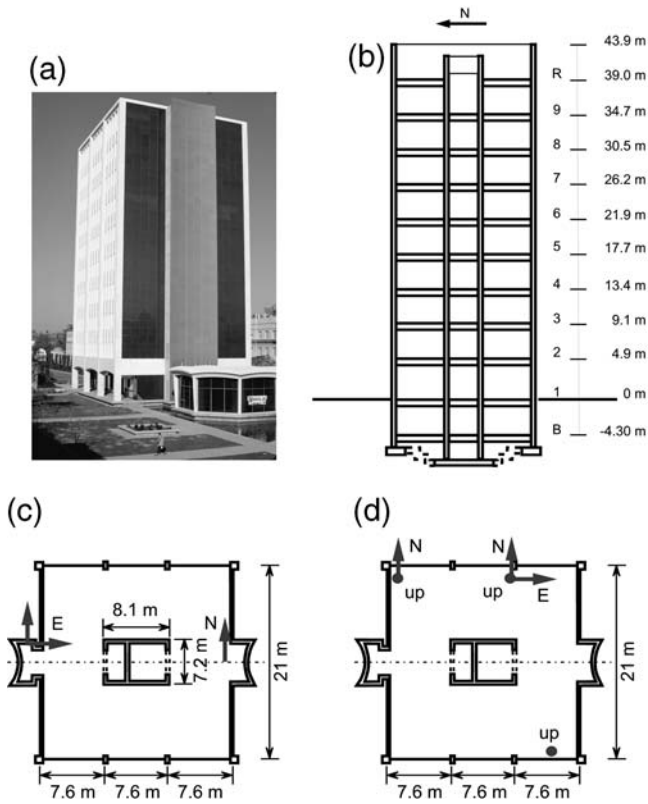


**Figure 1.** Millikan Library: (a) photo (taken by M.D. Trifunac), (b) vertical cross section, (c) typical floor layout (redrawn from Snieder and Şafak, 2006), and (d) sensor locations at basement.

The first earthquake recorded in the building was the Lytle Creek (LC) of 1970, which produced small amplitude response. It was followed by the San Fernando (SF) of 1971, which caused a significant drop of its resonant frequencies (Udwadia and Trifunac, 1974). Many other earthquakes were recorded in the building over the past 40 yr, most notably the Whittier–Narrows (WN) earthquake of 1987 ( $M$  5.9,  $R$  = 19 km), the Northridge earthquake of 1994 ( $M_L$  6.4,  $R$  = 34 km), and their aftershocks. At the time of this study, only data from five of the earthquakes were available both at basement and roof level. These earthquakes are listed in Table 1. Columns (2) through (9) show the earthquake name, date, magnitude, epicentral distance, roof peak acceleration, roof

peak velocity, and the rocking angle (sum of rigid-body rocking and rocking due to deformation of the structure). The Lytle Creek and San Fernando earthquakes were recorded by two triaxial RFT-250 accelerometers installed in 1968 (analog, located at the basement and roof), the Whittier–Narrows earthquake on a 10-channel CR-1 structural array installed in 1979 and operated by the Caltech Civil Engineering department (analog, sensors located at the basement, sixth floor and roof), and of the Yorba Linda and San Simeon (SS) earthquakes by a 36-channel digital structural array installed in 1998 and operated by U.S. Geological Survey (Clinton *et al.*, 2006). Figure 1c shows the sensor orientation on the floors above the basement, and Figure 1d in the basement. An additional triaxial accelerometer is installed on the ninth floor near the uniaxial sensor on the east side (not shown in this figure).

## Methodology

The methodology for estimation of the fixed-base and rigid-body rocking frequencies is described in detail in Todorovska (2009) and is reviewed here only briefly for completeness. The fixed-base frequency  $f_1$  is estimated using the relation

$$f_1 = 1/(4\tau), \quad (1)$$

where  $\tau$  is the wave travel time from the base to the top of the structure measured from impulse response functions. This relation is based on the assumption that the building deformation is primarily in shear, and that its stiffness and mass are distributed uniformly along the height. The rigid-body rocking frequency  $f_R$  is estimated based on the relation (Luco *et al.*, 1987)

$$\frac{1}{f_{1,\text{sys}}^2} \approx \frac{1}{f_H^2} + \frac{1}{f_R^2} + \frac{1}{f_1^2}, \quad (2)$$

where  $f_H$  and  $f_R$  are the horizontal and rocking rigid-body frequencies, and  $f_{1,\text{sys}}$  is the fundamental system frequency. If  $f_H \rightarrow \infty$  (infinite foundation horizontal stiffness), then  $f_{1,\text{sys}} \rightarrow f_{1,\text{app}}$  is the apparent building frequency. This special case of equation (2) is

**Table 1**  
Earthquakes Recorded in Millikan Library by a Structural Array for Which Records Are Available and Were Used in This Study

Number	Name	Data Source	Date	$M$	$R$ km	Roof Peak Acceleration cm/sec <sup>2</sup>	Roof Peak Velocity cm/sec <sup>2</sup>	$\theta_{\text{max}}$ 10 <sup>-3</sup> rad
(1)	(2)	(3)	(4)	(5)	(6)	(7)	(8)	(9)
1	Lytle Creek	Caltech	9/12/70	5.3	57	54	4.1	0.065
2	San Fernando	Caltech	2/9/71	6.6	31	301	25	0.516
3	Whittier–Narrows	CDMG	10/1/87	6.1	19	534	64	1.866
4	Yorba Linda	USGS	9/3/02	4.8	40	6.8	0.58	0.012
5	San Simeon	USGS	12/22/03	6.4	323	14.2	1.92	0.035

$$\frac{1}{f_{1,app}^2} \approx \frac{1}{f_R^2} + \frac{1}{f_1^2}. \quad (3)$$

Equation (2) is based on the assumption that the foundation is rigid. Frequency  $f_{1,app}$  is estimated from the peaks of the transfer function between the roof response and the response of the building at ground level, which corresponds to the condition  $f_H \rightarrow \infty$ . Given  $f_1$  and  $f_{1,app}$ ,  $f_R$  is computed from equation (3).

The wave travel time  $\tau$  is measured from impulse response functions obtained by deconvolution of the roof motion with the motion of the ground (Snieder and Şafak, 2006)

$$h(t; \xi = H) = \text{FT}^{-1}\{\hat{u}(\omega; \xi = H)/\hat{u}_{\text{ref}}(\omega)\}(t) \quad (4)$$

with  $\hat{u}_{\text{ref}}(\omega)$  being the Fourier transform response at ground level,  $\hat{u}(\omega; \xi)$  being the Fourier transform of the response at some level  $\xi$  measured from ground level, and  $\text{FT}^{-1}$  indicates inverse Fourier transform. Then  $h(t; \xi = H)$  corresponds to the roof response to excitation that results in horizontal impulse at ground level (ideally a Dirac delta-function  $\delta(t)$ ). Because  $\delta(t)$  is zero at all  $t$  except at  $t = 0$ , this corresponds to zero horizontal motion of the foundation, that is,  $f_H \rightarrow \infty$  but  $f_R < \infty$  (Todorovska, 2009). For the earthquake records, a regularized version of equation (4) was used (Snieder and Şafak, 2006)

$$\begin{aligned} h(t; \xi = H) \\ = \text{FT}^{-1}\{(\hat{u}(\omega; \xi = H) \bar{\hat{u}}_{\text{ref}}(\omega))/(|\hat{u}_{\text{ref}}(\omega)|^2 + \varepsilon)\}(t), \end{aligned} \quad (5)$$

where  $\varepsilon$  is the regularization parameter.

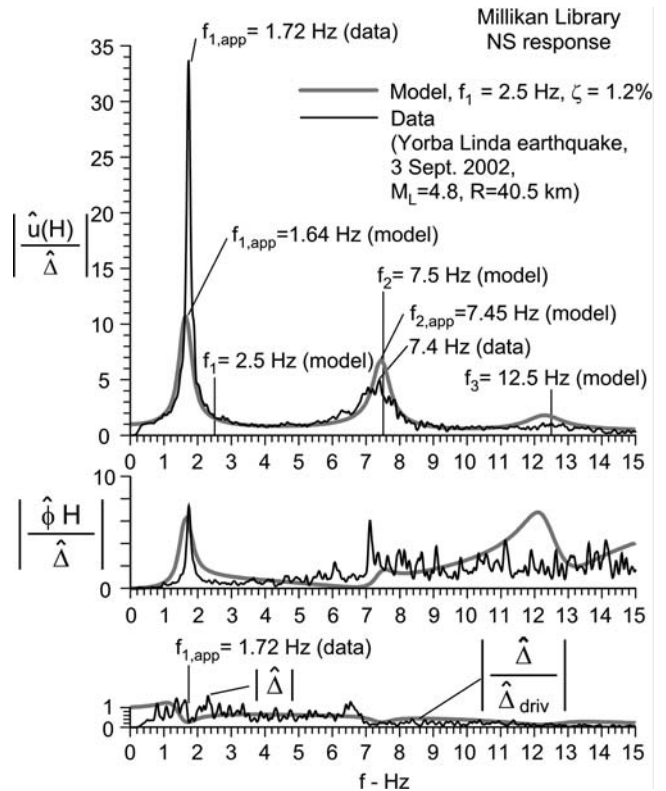
## Results and Analysis

### Comparison of Model and Experimental System Functions

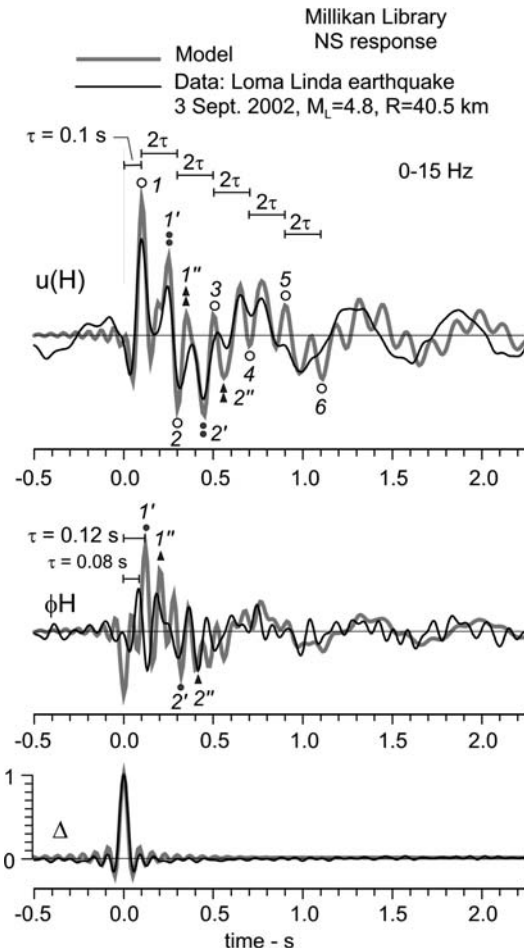
The following describes the model and measured transfer functions and impulse response functions for the north–south response of Millikan Library for small amplitude response. The measured response was computed using strong-motion data recorded in the building during the Yorba Linda earthquake (see Table 1). The model and its parameters are the same as those in Todorovska and Al Rjoub (2006, 2008) and Todorovska (2009) chosen to correspond approximately to the north–south response of Millikan Library. In that model, the foundation is semicircular with radius  $a = 12$  m, and the soil is homogeneous elastic half-space with Poisson ratio 0.3 and shear wave velocity 300 m/sec. The building is a uniform shear beam 44 m high and with fundamental fixed-base frequency  $f_1 = 2.5$  Hz. In view of the simplicity of the model and that its input parameters were chosen to roughly correspond to the case study, the objective of this comparison is to demonstrate qualitative agreement of the system functions.

Figure 2 shows comparison of the model and measured transfer-functions. In this figure,  $\Delta_{\text{driv}}$  is the foundation horizontal driving motion,  $\Delta$  is the resultant horizontal displacement of the foundation at ground level (sum of the driving motion and motion due to feedback forces),  $\varphi$  is the foundation rocking, and  $H$  is the height to the top sensor (hence  $\varphi H$  represents the horizontal roof displacement due to foundation rocking). For these parameters, the model gave rigid-body rocking frequency  $f_R \approx 2.055$  Hz and apparent frequency  $f_{1,app} \approx 1.64$  Hz. To mimic closely the model, the transfer functions for the earthquake data were computed from the roof and ground floor (averages of the motions at the east and west walls), which gave apparent frequency  $f_{1,app} \approx 1.72$  Hz. The foundation rocking however was computed from the vertical motions recorded at basement level (on the east side of the building), as there were no vertical sensors at the ground floor. It can be seen that there is good qualitative agreement between the approximate theoretical and observed transfer functions.

Figure 3 compares theoretical and experimental impulse response functions for input impulse at ground level. Both were obtained from transfer functions windowed between 0 and 15 Hz for a meaningful comparison because the earth-



**Figure 2.** Model (thick line) versus Yorba Linda 2002 earthquake (thin line) north–south response: transfer functions of roof response (top), and base rocking response (middle) with respect to horizontal response of ground level. The plot in the bottom shows the model horizontal response at ground level for unit driving motion (thick line) and the Fourier spectrum of the earthquake response at ground level (thin line) on a relative scale.



**Figure 3.** Model (thick line) versus Yorba Linda 2002 earthquake (thin line) north–south response: impulse responses of roof (top) and base rocking (middle) to input impulse at ground level (bottom), that is, roof horizontal motion, foundation rocking, and ground level horizontal motions deconvolved with the resultant horizontal motion at ground level.

quake did not excite the higher modes. It can be seen that there is good agreement also between the time domain system functions. The impulse first arrivals in the horizontal roof responses agree well and give wave travel time between ground level and roof  $\tau \approx 0.1$  s. The slight shift in the apparent frequencies (1.64 Hz for the model as compared to 1.72 Hz for the data, see Fig. 2) produces an increasing with time phase shift between the waveforms of the oscillatory part of the impulse response functions.

The theoretical first arrival of the input pulse at the roof is at  $t = 0.1$  sec and with the same sign. The second arrival is at  $t = 0.3$  sec  $= \tau + 2\tau$  following reflection from the base and sign reversal. The third arrival is at  $t = 0.5$  sec  $= \tau + 2\tau + 2\tau$  following another reflection from the base and sign reversal, etc. These pulses in Figure 3 are marked by open circles and numerals 1, 2, 3, etc. The ripples in between, which occur as pairs of pulses with same sign, marked by double symbols and numerals 1' and 1'', and 2' and 2'', etc., were explained in Todorovska (2009) to have been ra-

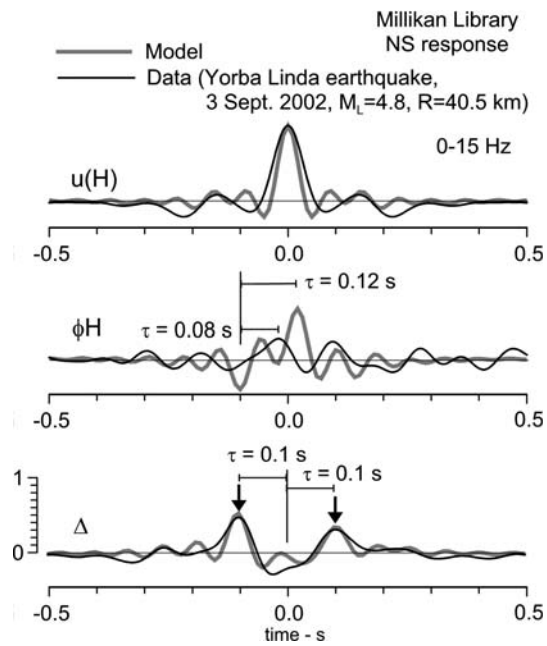
diated by rocking motion of the foundation, which are a result of feedback forces from the structure. These sources of the secondary pulses are marked in the impulse response of  $\varphi H$  by single symbols and numerals 1' and 1'', and as 2' and 2''. They occur as a result of reflections of the main pulses from the roof and foundation and have the same sign as the incident pulses on the corresponding boundary. Hence, pulse 1' in  $\varphi H$  is created shortly after pulse 1 in  $u(H)$  at  $t = \tau$ , and pulse 1'' is created with a delay  $\tau$ , that is, shortly after  $t = 2\tau$ . Pulses 1' and 1'' in  $u(H)$  occur with delay  $\tau$  relative to the corresponding pulses in  $\varphi H$ . In principle, each of these secondary arrivals at the roof will further generate feedback motions of the foundation, which will act as sources of waves, but these are difficult to recognize in the filtered impulse response functions. As it can be seen from Figure 3 in the observed impulse response function of  $\varphi H$ , 1', and 1'', etc., occur shortly before the causative pulses (e.g., pulse 1' occurs at  $t = 0.08$  sec, while its cause occurs at  $t = 0.1$  sec). This violation of causality appears to be caused because the foundation of the actual building is not absolutely rigid (hence, it takes some time for a wave to propagate from the basement to the ground floor), because the rocking was computed from the basement records, while the virtual source is at the ground floor, and possibly also because the sensors at the basement are not along the same vertical line with the sensors at ground and roof levels.

Figure 4 compares theoretical and experimental impulse response functions for input impulse at the roof. For the same reasons stated elsewhere (Snieder and Şafak, 2006; Todorovska, 2009), the reflections from the roof are suppressed, which simplifies the waveforms of the impulse responses, and there is an acausal arrival at the ground floor at  $t = -0.1$  sec besides a causal one at  $t = 0.1$  sec because the physical source of waves is at the basement.

The close resemblance of the model (based on homogeneous shear beam) and observed roof impulse responses at least up to five reflections of the input pulse suggests that internal reflections of waves from the floor slabs and dispersion are not significant for the north–south response of this building at least in the frequency band 0–15 Hz.

#### Fixed-Base, Rigid-Body and Apparent Frequencies during Earthquakes

Figure 5 shows the building response versus time (as the rocking  $\theta(t)$ ) during the five earthquakes listed in Table 1. This angle was computed as the difference between the roof and basement horizontal response divided by the distance between the basement and roof sensors. Therefore, it is not entirely due to deformation of the structure but includes the rigid-body rocking, which could not be separated for the earlier earthquakes. This angle can be used as an estimate of the average drift of the building (including drift due to rigid-body rocking). For example,  $\theta(t) = 10^{-3}$  rad corresponds to drift of 0.1%. It can be seen that the Yorba Linda earthquake caused the smallest response and the Whittier–



**Figure 4.** Model (thick line) versus Yorba Linda 2002 earthquake (thin line) north–south response: impulse responses of base rocking (middle) and ground level horizontal response (bottom) to input impulse at roof level (top), that is, roof horizontal motion, foundation rocking, and ground level horizontal motions deconvolved with the roof horizontal motion.

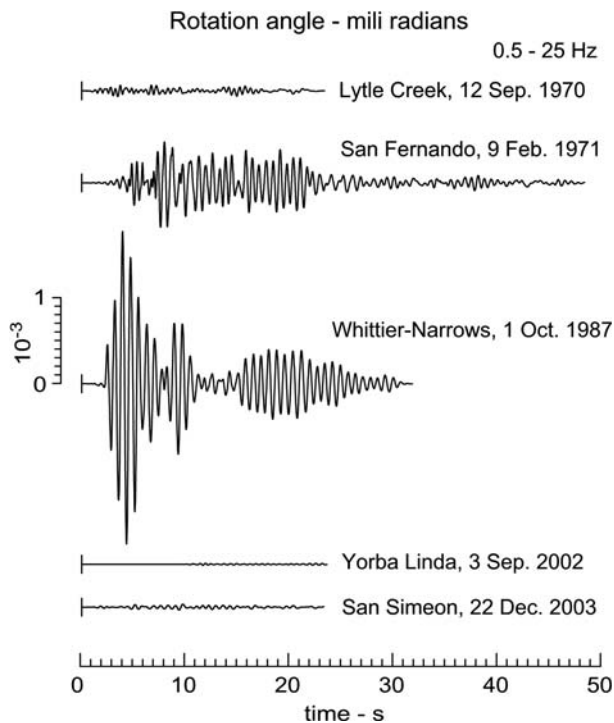


**Figure 5.** Roof north–south rocking angle (sum of rigid-body rocking and rocking due to elastic deformation).

Narrows—the largest of the five earthquakes. While with twice smaller amplitudes, the building response during the San Fernando earthquake was the first significant response since construction.

For each earthquake, the apparent frequency  $f_{1,app}$  was measured from the first peak of the transfer function between roof and basement responses, the fixed-base frequency  $f_1$  was estimated from the wave travel time  $\tau$  between basement and roof as  $f_1 = 1/(4\tau)$ , and an estimate of the rocking frequency  $f_R$  was then computed based on equation (3). The wave travel time was read from interpolated impulse response functions. For the San Fernando earthquake, these frequencies were computed for six segments (SF1: 0–3.5 sec, SF2: 3–6.5 sec, SF3: 6.5–10 sec, SF4: 10–15 sec, SF5: 15–22 sec, and SF6: 22–50 sec), and for the Whittier–Narrows earthquake for three segments (WN1: 2.2–7.2 sec, WN2: 7.2–15 sec, and WN3: 15–30 sec). Because of narrowband nature of the responses, the impulse response functions did not yield reliable reading of the wave travel time  $\tau$  (and  $f_1$ ) for the San Simeon earthquake, for segment SF5 of the San Fernando earthquake, and for segments WN2 and WN3 of the Whittier–Narrows earthquake (see discussion and examples in Todorovska, 2009). Consequently, the corresponding estimates of  $f_1$  and  $f_R$  are not shown. Further, because segment SF1 is very short compared to the other segments (3.5 sec), its localization in frequency is associated with much larger uncertainty (due to the Heisenberg–Gabor uncertainty principle).

The results are summarized in Table 2. In this table, columns (1) to (12) show the code for the earthquake/interval, the wave travel time  $\tau$ , the fixed-base frequency  $f_1$ , apparent frequency  $f_{1,app}$ , rocking frequency  $f_R$ , peak roof acceleration, peak roof velocity, peak rocking angle  $\theta_{max}$ , peak drift, and percentage changes in  $f_1$ ,  $f_{1,app}$ , and  $f_R$ , relative to their values during the Lytle Creek earthquake. It can be seen that, for this set of earthquakes,  $0.07 \text{ mrad} < \theta_{max} < 1.87 \text{ mrad}$ . The peak drift during the San Fernando earthquake was 0.052%, and during Whittier–Narrows earthquake it was 0.187%, which approaches but is less than the drift considered to cause damage of moment resistant frames (0.2%; Ghobarah, 2004). The range of frequencies and percentage change are as follows:  $2.12 \text{ Hz} < f_1 < 3.05 \text{ Hz}$  (30% variation),  $1.44 \text{ Hz} < f_R < 2.47 \text{ Hz}$  (42% variation), and  $1.19 \text{ Hz} < f_{1,app} < 1.92 \text{ Hz}$  (38% variation).

The results are presented graphically in Figures 6 through 9. Figures 6, 7, and 8 show  $f_1$ ,  $f_R$ , and  $f_{1,app}$  versus  $\theta_{max}$ , while Figure 9 shows a correlation plot of the percentage changes in  $f_R$  and  $f_1$ . Each data point is represented by the corresponding symbol for the earthquake/segment.

Figure 6 shows that  $f_1$  dropped by 24% during the first 10 sec of shaking by the San Fernando earthquake (segments SF2 and SF3) and increased slightly during the subsequent smaller amplitude response. It further dropped during the first 7 sec of the Whittier–Narrows earthquake but much less (by 8.5%) considering the large increase in amplitudes of response ( $\theta_{max}$  reaching 1.87 mrad) and recovered with de-

Table 2  
Wave Travel Time from Basement to Roof, Frequencies, Peak Roof Responses, and Changes in Frequencies Relative to the Lytle Creek 1970 Earthquake

Earthquake	$\tau$ sec	$f_1$ Hz	$f_{1,app}$ Hz	$f_R$ Hz	Roof Peak Acceleration cm/sec <sup>2</sup>	Roof Peak Velocity cm/sec <sup>2</sup>	$\theta_{max}$ 10 <sup>-3</sup> rad	Drift %	$\frac{\Delta f_1}{f_1}$ %	$\frac{\Delta f_{1,app}}{f_{1,app}}$ %	$\frac{\Delta f_R}{f_R}$ %
(1)	(2)	(3)	(4)	(5)	(6)	(7)	(8)	(9)	(10)	(11)	(12)
LC	0.08	3.05	1.92	2.47	54	4	0.07	0.007	0.0	0.0	0.0
SF1	0.08	3.01	1.76	2.17	36	3	0.05	0.005	-1.2	-8.3	-12.3
SF2	0.10	2.63	1.70	2.23	200	14	0.26	0.026	-13.7	-11.5	-9.9
SF3	0.11	2.31	1.55	2.09	301	25	0.52	0.052	-24.1	-19.3	-15.6
SF4	0.11	2.31	1.52	2.02	192	20	0.38	0.038	-24.1	-20.7	-18.2
SF5	0.11	2.31	1.57	2.14	167	17	0.39	0.039	-24.1	-18.2	-13.6
SF6	0.11	2.38	1.61	2.19	56	7	0.14	0.014	-21.9	-16.2	-11.6
WN1	0.12	2.12	1.19	1.44	534	64	1.87	0.187	-30.5	-38.0	-41.8
WN2	-	-	1.35	-	246	28	0.82	0.082	-	-29.7	-
WN3	-	-	1.36	-	131	16	0.41	0.041	-	-29.2	-
YL	0.11	2.38	1.71	2.46	7	0.6	0.01	0.001	-21.9	-11.0	-0.8
SS	-	-	1.62	-	14	1.9	0.04	0.004	-	-15.6	-

creasing response during the small amplitude Yorba Linda earthquake following practically the same path. The two trends of variation of  $f_1$  versus  $\theta_{max}$  are shown by thick, fuzzy lines drawn by hand (the first through points LC, SF1, SF2, and SF3 and the second through points SF4, SF6, WN1, and YL), which indicate permanent change in  $f_1$  due to structural degradation caused by the San Fernando earthquake and amplitude dependent and mostly recoverable (within the accuracy of the estimates) change of  $f_1$  for the cracked structure during the subsequent earthquakes. Hence, no significant additional degradation of stiffness occurred during the Whittier–Narrows earthquake.

Figure 7 shows that  $f_R$  decreased by 18% with increasing  $\theta_{max}$  during the first 10 sec of shaking by the San Fernando earthquake (segments SF2 and SF3) continued to decrease during segment SF4, although  $\theta_{max}$  decreased and

recovered partially during segments SF6, as  $\theta_{max}$  continued to decrease. During the Whittier–Narrows earthquake, it dropped markedly by 30% and recovered during the Yorba Linda earthquake approximately to its value during the Lytle Creek earthquake. This pattern suggests that in the long term,  $f_R$  recovered completely, but the recovery was not instantaneous (as for  $f_1$ , see Fig. 6) following the strong shaking during the initial 10 sec of the response to the San Fernando earthquake. The total change of  $f_R$  was 42%.

Figure 8 shows that  $f_{1,app}$  dropped during the San Fernando earthquake and recovered partially toward the end of shaking. Then it dropped further during the initial 7 sec of the response to the Whittier–Narrows earthquake recovered partially toward the end of the shaking and further recovered during the smaller Yorba Linda and San Simeon earthquakes. The total change of  $f_{1,app}$  was 38%.

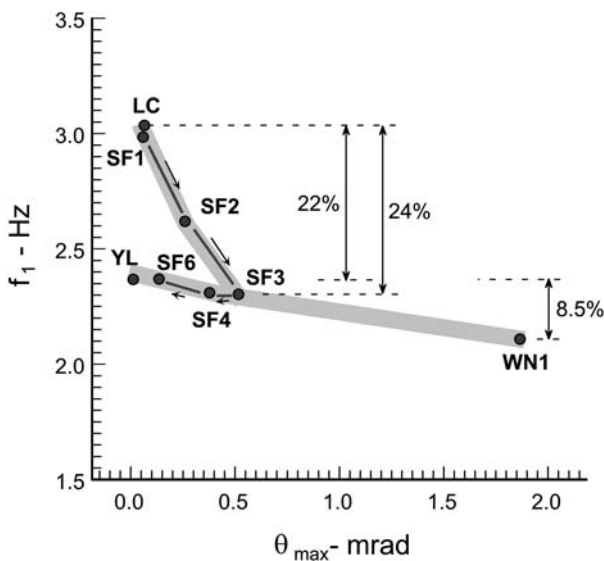


Figure 6. Fixed-base frequency (north–south) versus level of response.

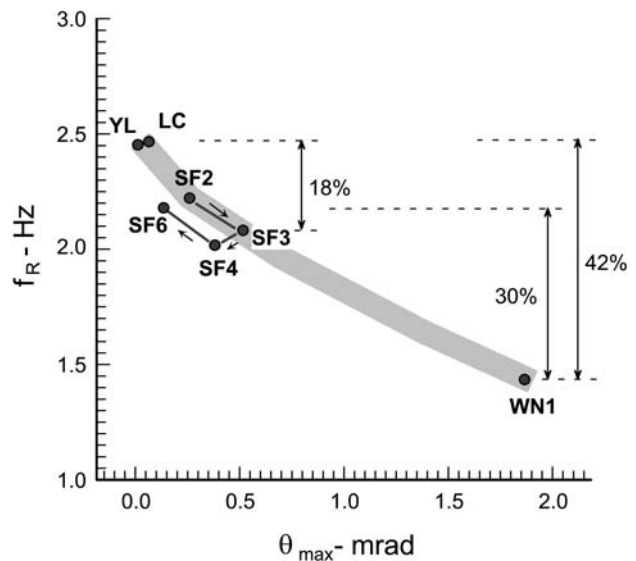
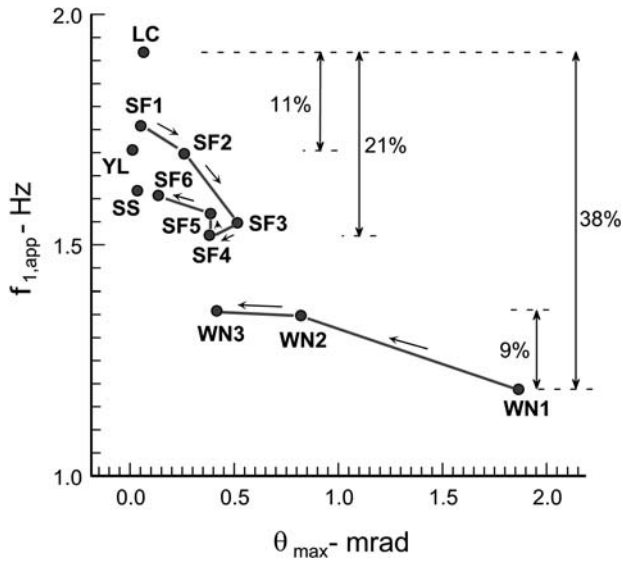
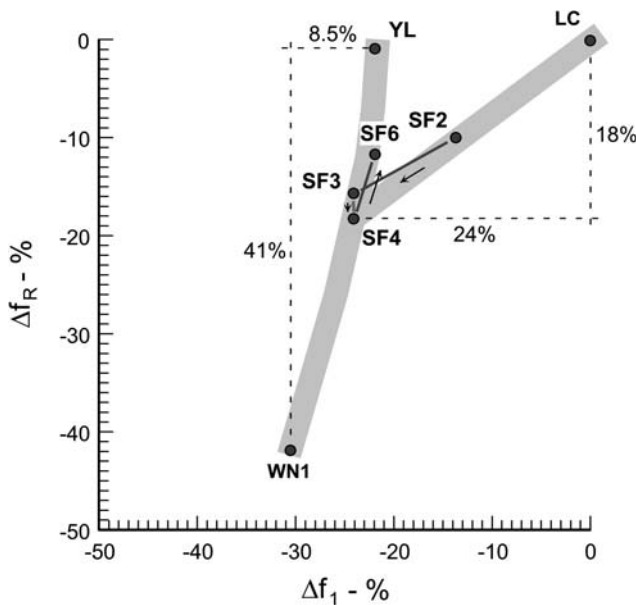


Figure 7. Rigid-body rocking frequency (north–south) versus level of response.



**Figure 8.** Apparent frequency (north-south) versus level of response.

The data from the Lytle Creek and Yorba Linda earthquakes, which caused similar amplitude responses, give an opportunity to examine permanent changes in  $f_1$ ,  $f_R$ , and  $f_{1,app}$  over the period from 1970 to 2002. The data show no change of  $f_R$ , change in  $f_1$  of  $-22\%$ , and change in  $f_{1,app}$  of  $-11\%$ . The much smaller change in  $f_{1,app}$ , which represents the combined effect of change in  $f_1$  and  $f_R$ , compared to the change in  $f_1$  alone, is due to the nature of their combination rule (see equation 3). These changes in  $f_1$  and  $f_{1,app}$  correspond to about  $-39\%$  change in the overall structural stiffness and about  $-21\%$  change in the equivalent stiff-



**Figure 9.** Percentage change of rocking frequency (north-south) versus percentage change of fixed-base frequency (north-south) for four earthquakes.

ness of the structure and the rocking soil spring. Hence, observing change in  $f_{1,app}$  instead of  $f_1$  will underestimate the changes in structural stiffness.

An interesting question is to what degree the observed changes in  $f_{1,app}$  of this building have been due to changes in  $f_1$  as opposed to  $f_R$  during the San Fernando earthquake and after. Figure 9 shows that, between the Lytle Creek earthquake and San Fernando earthquake (segment SF4),  $f_1$  dropped by  $24\%$ , and  $f_R$  dropped by  $18\%$ , while  $f_{1,app}$  dropped by  $21\%$  (see Fig. 8). Between the Whittier–Narrows earthquake (segment WN1) and the Yorba Linda earthquake,  $f_1$  changed (recovered) by  $8.6\%$ ,  $f_R$  by  $41\%$ , while  $f_{1,app}$  by  $27\%$ . This suggests that  $f_1$  and  $f_R$  changed comparably during the San Fernando earthquake when degradation of the structural stiffness occurred (with the change in  $f_1$  being slightly larger), while after the San Fernando earthquake, the observed changes in  $f_{1,app}$  have been to a much larger degree (by a factor of almost 5) due to changes in  $f_R$ .

#### Comparison with Results from Forced Vibration Tests

Luco *et al.* (1987) and *et al.* Wong (1988) performed system identification of Millikan Library from forced vibration data from a test conducted in 1975 after the San Fernando earthquake (Foutch *et al.*, 1975) and report for the north-south response:  $f_1 = 2.33$  Hz,  $f_R = 3.01$  Hz, and  $f_H = 7.51$  Hz. The identification analysis in this article gives for the response during the Yorba Linda earthquake of 2002:  $f_1 = 2.38$  Hz,  $f_R = 2.46$  Hz, and  $f_H = 9.01$  Hz. Here,  $f_H$  was obtained from  $f_{1,sys} = 1.68$  Hz (read from the smoothed Fourier spectrum of the roof acceleration response) and  $f_{1,app} = 1.71$  Hz (read from the smoothed transfer-function between roof and basement response as in Table 2) based on equations (2) and (3), and  $f_1$  was obtained from wave travel time between basement and roof. Considering the finite accuracy of both system identifications, these estimates are in close agreement. Note that in Figures 2 and 3 the ground floor record was used as reference.

Clinton *et al.* (2006) summarize results for  $f_{1,sys}$  during eight forced vibration tests between 1967 and 2002, eight earthquakes between 1970 and 2003, and continuous stream of ambient vibration data recorded between 2001 and 2003. The measurements from the forced vibration tests, which involve similar amplitude response, make it possible to analyze the long-term trends. Using the value of the 1967 test as reference ( $f_{1,sys} = 1.90$  Hz), these tests suggests drop of  $6.8\%$  due to the San Fernando earthquake,  $3.7\%$  due to the Whittier–Narrows earthquake, and  $1.6\%$  due to the Northridge earthquake. The total change between 1967 and 2002 is  $13.7\%$  and  $12.1\%$  (based on two tests with different shaker weights), which is close to the total change in  $f_{1,app}$  of  $11\%$  between the 1970 Lytle Creek and the 2002 Yorba Linda earthquake determined by this study.

## Discussion and Conclusions

The trends in the variations of the north–south fixed base ( $f_1$ ) and rigid-body rocking ( $f_R$ ) frequencies of Millikan Library during four earthquakes (1970–2002) suggest the following. All quoted variations are relative to the values during the Lytle Creek earthquake of 1970.

- (1) *Permanent changes:* The north–south fixed-base frequency,  $f_1$ , dropped permanently during the San Fernando earthquake of 1971 (peak drift 0.052%), suggesting degradation of structural stiffness caused by the earthquake (in agreement with Luco *et al.*, 1987). After this earthquake, it did not experience any significant permanent changes even during the much larger response during the Whittier–Narrows earthquake (peak drift 0.187%). The permanent change of  $f_1$  between 1970 and 2002 as measured from the Lytle Creek and Yorba Linda earthquakes, which produced similar response amplitudes, was about 22%. Assuming no change in mass, 22% in  $f_1$  implies 49% change in structural stiffness, between the virgin state in 1970 and the experienced state in 2002 (following exposure to two significant earthquakes) even though there was no serious damage. The corresponding change in  $f_{1,app}$  is about 11% (implying reduction of system stiffness by 23%), while  $f_R$  remained approximately the same. The change is larger in  $f_1$  than in  $f_{1,app}$  because of the nature of the combination rule between  $f_1$ ,  $f_R$  and  $f_{1,app}$ .
- (2) *Range of the variation over the four earthquakes:* The rigid-body rocking frequency,  $f_R$ , varied significantly from one earthquake to another with maximum variation of about 42%, but all changes were amplitude dependent and recoverable. The fixed-base frequency,  $f_1$ , also varied as function of amplitude but to a smaller degree. The maximum variation of  $f_1$  was about 30% and of  $f_{1,app}$  was about 38%. Both  $f_1$  and  $f_R$  were the lowest during the Whittier–Narrows earthquake of 1987, which apparently did not cause any significant degradation of the structural stiffness.
- (3) *What caused the observed change in  $f_{1,app}$  during the San Fernando earthquake?* During the San Fernando earthquake,  $f_1$  dropped by about 24%, and  $f_R$  dropped by about 18%, while their combined effect on the apparent frequency,  $f_{1,app}$ , was a drop by 20.7%. Hence, changes in  $f_R$  (soil) and  $f_1$  (structure) contributed comparably to the observed drop in  $f_{1,app}$  with the latter change being slightly larger.
- (4) *What caused the observed change in  $f_{1,app}$  after the San Fernando earthquake?* After the San Fernando earthquake, the variations of both  $f_1$  and  $f_R$  appear to be amplitude dependent and recoverable. Their variations are the largest between the strong motion segment of the Whittier–Narrows earthquake (WN1) and the subsequent Yorba Linda earthquake. Between these two earthquakes,  $f_1$  changed by 8.6%,  $f_R$  by 41%, and  $f_{1,app}$

by 27%. Hence, after the San Fernando earthquake, the observed changes in  $f_{1,app}$  have been to a much larger degree (almost 5 times) due to changes in  $f_R$  than  $f_1$ .

- (5) *Was the recovery of  $f_1$  and  $f_R$  instantaneous?* A comparison of the trends of recovery during the San Fernando earthquake (toward the end of shaking, Figs. 6 and 7) with the trends of variation of  $f_1$  and  $f_R$  with amplitudes of response indicates that the recovery of  $f_1$  is instantaneous, while that of  $f_R$  is gradual consistent with a longer term healing process of the soil (previously suggested for a different building by Trifunac *et al.*, 2001a, b).

The analysis and conclusions of this study are preliminary and based on data from only four earthquakes. Other earthquakes have also been recorded, for example, Sierra Madre 1988  $M$  5.8,  $R = 18$  km; Northridge 1994  $M$  6.7,  $R = 34$  km, and its aftershocks; Beverly Hills 2001  $M$  4.2,  $R = 26$  km listed in Clinton *et al.* (2006). The Landers ( $M$  7.5) and Big Bear ( $M$  6.5) earthquakes of 1992 should have also been recorded. Unfortunately, Caltech has not so far released data recorded by the CR-1 array after 1987. Once these and other future earthquake records become available, it will be possible to refine and to verify the trends discussed in this article.

## Data and Resources

All data used for this study are publicly available. The digitized records of the Lytle Creek and San Fernando earthquakes were made available to the author by M. D. Trifunac. Data from the San Fernando earthquake are also available from the Center for Engineering Strong Motion Data Web site ([www.strongmotioncenter.org](http://www.strongmotioncenter.org), last accessed November 2008) of the Whittier–Narrows earthquake by the California Geological Survey (on floppy disks), and of the Yorba Linda and San Simeon earthquakes by the U.S. Geological Survey USGS National Strong Motion Program ([nsmf.wr.usgs.gov](http://nsmf.wr.usgs.gov), last accessed November 2008).

## References

- Clinton, J. F., S. K. Bradford, T. H. Heaton, and J. Favela (2006). The observed wander of the natural frequencies in a structure, *Bull. Seismol. Soc. Amer.* **96**, no. 1, 237–257.
- Foutch, D. A., J. E. Luco, M. D. Trifunac, and F. E. Udawadia (1975). Full scale three-dimensional tests of structural deformations during forced excitation of a nine-story reinforced concrete building, *Proc. of the U.S. National Conf. on Earthquake Engineering*, Ann Arbor, Michigan, 206–215.
- Ghobarah, A. (2004). On drift limits associated with different damage levels, *Proc. of the International Workshop on Performance-Based Seismic Design Concepts and Implementation*, Bled, Slovenia, 28 June–1 July 2004, P. Fajfar and H. Krawinkler (Editors), PEER Rept. 2004/05, Pacific Earthquake Engineering Research Center, University of California, Berkeley, California.
- Kawakami, H., and M. Oyunchimeg (2004). Wave propagation modeling analysis of earthquake records for buildings, *J. Asian Arch. Bldg. Eng.* **3**, no. 1, 33–40.

- Luco, J. E., H. L. Wong, and M. D. Trifunac (1986). Soil-structure interaction effects on forced vibration tests, *Technical Rept. CE86-05*, Department of Civil Engineering, University of Southern California, Los Angeles, California.
- Luco, J. E., M. D. Trifunac, and H. L. Wong (1987). On the apparent change in the dynamic behavior of a nine-story reinforced concrete building, *Bull. Seismol. Soc. Am.* **77**, no. 6, 1961–1983.
- Luco, J. E., M. D. Trifunac, and H. L. Wong (1988). Isolation of soil-structure interaction effects by full-scale forced vibration tests, *Earthq. Eng. Struct. Dyn.* **16**, 1–21.
- Snieder, R., and E. Şafak (2006). Extracting the building response using interferometry: theory and applications to the Millikan Library in Pasadena, California, *Bull. Seismol. Soc. Am.* **96**, no. 2, 586–598.
- Todorovska, M. I. (2009). Seismic interferometry of a soil-structure interaction model with coupled horizontal and rocking response, *Bull. Seismol. Soc. Am.*, **99**, no. 2A, 611–625.
- Todorovska, M. I., and Y. Al Rjoub (2006). Effects of rainfall on soil-structure system frequency: examples based on poroelasticity and a comparison with full-scale measurements, *Soil Dyn. Earthq. Eng.* **26**, no. 6–7, 708–717.
- Todorovska, M. I., and Y. Al Rjoub (2008). Environmental effects on measured structural frequencies—model prediction of short term shift during heavy rainfall and comparison with full-scale observations, *Struct. Control Health Monit.*, in press, doi 10.1002/stc.260.
- Todorovska, M. I., and M. D. Trifunac (2008a). Earthquake damage detection in the Imperial County Services Building III: analysis of wave travel times via impulse response functions, *Soil Dyn. Earthq. Eng.* **28**, no. 5, 387–404 doi 10.1016/j.soildyn.2007.07.001.
- Todorovska, M. I., and M. D. Trifunac (2008b). Impulse response analysis of the Van Nuys 7-storey hotel during 11 earthquakes and earthquake damage detection, *Struct. Control Health Monit.* **15**, no. 1, 90–116, doi 10.1002/stc.208.
- Todorovska, M. I., M. D. Trifunac, and T. Y. Hao (2006). Variations of apparent building frequencies—lessons from full-scale earthquake observations, *Proc. of the First European Conference on Earthquake Engineering (ECEE) and Seismology*, a joint event of the 13th ECEE and 30th General Assembly of the European Seismological Commission, Geneva, Switzerland, 3–8 September 2006, Paper No. 1547, 9 pp.
- Trifunac, M. D., S. S. Ivanović, and M. I. Todorovska (2001a). Apparent periods of a building I: Fourier analysis, *J. Struct. Eng.*, American Association of Civil Engineers, **127**, no. 5, 517–526.
- Trifunac, M. D., S. S. Ivanović, and M. I. Todorovska (2001b). Apparent periods of a building II: time-frequency analysis, *J. Struct. Eng.* ASCE, **127**, no. 5, 527–537.
- Trifunac, M. D., M. I. Todorovska, M. I. Manić, and B. D. Bulajić (2008). Variability of the fixed-base and soil-structure system frequencies of a building—the case of Borik-2 building, *Struct. Control Health Monit.*, in press, doi 10.1002/stc.277.
- Udwadia, F. E., and M. D. Trifunac (1974). Time and amplitude dependent response of structures, *Earthq. Eng. Struct. Dyn.* **2**, 359–378.
- Wong, H. L., M. D. Trifunac, and J. E. Luco (1988). A comparison of soil-structure interaction calculations with results of full-scale forced vibration tests, *Soil Dyn. Earthq. Eng.* **7**, no. 1, 22–31.

Department of Civil and Environmental Engineering  
University of Southern California  
Los Angeles, California 90089-2531  
mtodorov@usc.edu

Manuscript received 27 February 2008